Communications on Applied Nonlinear Analysis
ISSN: 1074-133X
Vol 32 No. 9s (2025)

A Study of Bioconvective Williamson Fluid of an Exponential Stretching Sheet with Chemical Reaction

M. R. Mishra[a*], S. Singh[b], D. Samal[c]

[a,b,c]Department of Mathematics, O.P. Jindal University, Raigarh, 496001 India

*Corresponding Author E-mail: mail_to_mrmishra@yahoo.co.in

Article History:

Received: 12-01-2025

Revised: 15-02-2025

Accepted: 01-03-2025

Abstract:
The present study's primary objective is to look into how thermophoresis diffusion and Brownian motion impacts the results of heat radiation and microorganism bioconvection in non-Newtonian Williamson fluid flow via exponentially stretched sheets. Similarity transformations have been applied in this case to transform PDEs into their corresponding ODEs. R-K method with shooting technique is applied to find the solution in a numerical approach. Fluid velocity increases with mixed convection and decreases with increasing magnetic parameter. The temperature grows as thermophoresis and Brownian motion parameters rise. The velocity field is declined by the effect bioconvection Lewis number (Bio. LNo.).

Keywords: Bioconvection, Williamson fluid, stretching sheet, chemical reaction.

1. Introduction

The influence of heat radiation and the bio-microorganism phenomena in MHD Williamson fluid flow on an exponentially stretching sheet are investigated in this study. Because of it's a variety of applications in the scientific and technological industrial sectors, as well as its growing capacity to transfer heat, researchers have taken an interest in the analysis over a stretching sheet of non-Newtonian fluid flow. In nuclear reactors, heat exchangers, solar systems, and other systems that include fluids and symmetrically extended sheets, the impact of HMT under the influence of chemical processes is crucial. [1–8].

A solution's microbe motility is the vital factor that drives the bioconvection process. Microbes react with different chemicals and density of other element by moving in certain directions. The variation among positive and negative microbe motility is caused by distortion in the stimulus's instruction for the opposite action. Because It's been demonstrated that bacteria have the potential to move up inside solution cells, gyrotactic microorganisms often migrate in response to a density difference. The only approach employed in bioremediation for removal of environmental pollutants from a location is the introduction of microorganisms. Researchers initially proposed a study on the importance of oxyntic and gyrotactic bacteria. [9-12]

Due to its various applications in glass fiber, plastic film, paper processing, metal drawing, stretching sheets have drawn substantial interest in the last few years. Recently, making use of stretching sheets, several researchers delved at the MHD flow and its many consequences, including chemical reactions and viscous dissipation. [13-22]

Chu et al. [23] shown the effects of thermal diffusion, activation energy (A.E.), Brownian motion, mobile microorganisms, and chemical reactions on the flow of a bioconvective MHD fluid related to stretching sheet. Mlamuli Dhlamini et. al. [24] developed the bio-convection flow's mathematical model and calculated the A.E. for chemical reactions. Computational techniques and algorithms for the irreversibility investigation of a blood nanofluid passing over an interface with A.E. and squeezing were developed by Naresh Kumar et al. [25] in the field of biomedicine.

Zafar et al. [26] studied chemical reactions and Prandtl nanofluid A.E. with bio-convection flow across a vertical surface. The viscosity that changes with temperature has been studied and the Arrhenius kinetic energy magnetized bioconvective nanofluid flow was numerically calculated by A. Shahid et. al. [27]. The effects of various thermal radiations as well as the Prandtl number on the MHD flow and thermal analysis of hybrid nanofluids were investigated by Sachin Shaw et. al. [28]. In a hybrid nanofluid flow (water based), researcher [29] used MHD and nonlinear radiation to simulate heat, entropy, and mass transfer. Using the bivariate spectral quasi-linearization approach, Oyelakin et al. [30] designed a Casson nanofluid that maximizes generation of entropy in unstable stagnating flows across a stretched sheet with Arrhenius A.E. and the chemical reaction.

The industrial sector uses Williamson fluids' pseudo-plastic boundary layers for emulsion-coated polymer sheets used in extrusion and high molecular weight polymer materials for photographic films. Various non-Newtonian models [31-35] have been used to study the dynamics of pseudo-plastic fluids, including as the power law, Cross, Carreaus, Ellis, and other models. However, an immense amount of research has been done on the various ways that Williamson fluid moves through a stretching surface where MHD is present.

Muhammad Imran Asjad et al. [36] investigated thermophoresis diffusion and Brownian motion in a Williamson fluid flow on a symmetrically stretched sheet. As a result, they identified that the Bio. LNo. Lb and Peclet number Pe caused the motile microbe profile to decline and the bioconvection Rayleigh number Rb to rise. Raising the suction/injection parameter s and the Williamson parameter We causes the coefficient of skin friction to decrease, whereas increasing the magnetic parameter M causes it to rise. R. Ahmed et al. [37] provided a depiction of this result. The rate of heat transmission increases as Pr grows, as shown by Ishak [16] and Goud et. al. [38]. The main goal of this context is to observe that, if adding heat radiation and bio-convection to Williamson magneto-hydrodynamics fluid flow using gyrotactic auto-motile microorganisms can lessen the chance of precipitation. These vital features give many contemporary technologies' heat exchange processes the necessary, favourable heat mobility, and their presence may be beneficial. [39-41].

2. Mathematical Formulation

Here x- and y-axes were assumed to be normal with velocity $\bar{U}_w = a_0 e^{x/l}$, and we studied steady incompressible MHD fluid flow through an exponentially stretching sheet in the present context. A magnetic field can be found in the flow zone that acts in the y-direction. Microorganisms and nanoparticles are gently dispersed throughout the liquid. When thermal radiation is taken into account, microorganism movement causes bioconvection to occur. $\bar{U}, \bar{V}$ are the fluid velocity for 2D fluid flow.

The Governing equations are.

$$\bar{U}_x + \bar{V}_y = 0 \tag{1}$$

$$\bar{U}\bar{U}_x + \bar{V}\bar{U}_y = \vartheta\bar{U}_{yy} + 2\vartheta\Gamma\bar{U}_y\bar{U}_{yy} - \frac{\sigma}{\rho}\left(M_0{}^2\bar{U}\right) + \frac{1}{\rho}\left[\xi\beta\rho\left(1-\bar{C}_\infty\right)\left(T-\bar{T}_\infty\right) - \xi\left(\rho_p-\rho_f\right)\left(\bar{C}-\bar{C}_\infty\right) - \xi\gamma\left(\rho_m-\rho_f\right)\left(\bar{N}-\bar{N}_\infty\right)\right] \tag{2}$$

$$\bar{U}\bar{T}_x + \bar{V}\bar{T}_y = \alpha\bar{T}_{yy} - \frac{1}{\rho C_p}\left(\frac{\partial q_r}{\partial y}\right) + \tau\left[D_B\bar{T}_y\bar{C}_y + \frac{D_T}{\bar{T}_\infty}\left(\bar{T}_y\right)^2\right] \tag{3}$$

$$\bar{U}\bar{C}_x + \bar{V}\bar{C}_y = D\bar{C}_{yy} - K_r{}^2\left(\bar{C}-\bar{C}_\infty\right)\left(\bar{T}/\bar{T}_\infty\right)^n e^{\left(-Ea/k\bar{T}\right)} + \frac{D_T}{\bar{T}_\infty}\bar{T}_{yy} \tag{4}$$

Bioconvection equation

$$\bar{U}\bar{N}_x + \bar{V}\bar{N}_y = \bar{N}_{yy}D_n - dW_c\frac{\partial}{\partial y}\left(\frac{\bar{N}}{\Delta\bar{C}}\bar{C}_y\right) \tag{5}$$

with the associated boundary conditions

$$\bar{U}(x,0) = \bar{U}_w,\ \bar{V}(x,0) = -\gamma(x),\ \bar{T}(x,0) = \bar{T}_w,\ \bar{C}(x,0) = \bar{C}_w,\ \bar{N}(x,0) = \bar{N}_w \tag{6}$$

$$\bar{U}\to 0,\ \bar{T}\to\bar{T}_\infty, \bar{C}\to\bar{C}_\infty, \bar{N}\to\bar{N}_\infty\ as\ y\to\infty$$

At this point, let's consider

$$\bar{U}_w = a_0e^{(x/l)},\ \gamma(x) = -V_0e^{(x/2l)},\ \bar{T}_w = \bar{T}_\infty + \bar{T}_0e^{(x/2l)}, \bar{C}_w = \bar{C}_\infty + \bar{C}_0e^{(x/2l)}, \bar{N}_w = \bar{N}_\infty + \bar{N}_0e^{(x/2l)} \tag{7}$$

By Rosseland approximation $q_r = \frac{4\sigma^*}{3k_1}\frac{\partial\bar{T}^4}{\partial y}$, and using the Taylor series, we have $\bar{T}_4 = 4\bar{T}_\infty{}^3\bar{T} - 3\bar{T}_\infty{}^4$

where $\bar{T}_\infty$, is the ambient temperature [42],

Eq. (3) can be written as

$$\bar{U}\bar{T}_x + \bar{V}\bar{T}_y = \bar{T}_{yy}\left[\alpha + \frac{16\sigma^*\bar{T}_\infty{}^3}{3k_1\rho C_p}\right] + \tau\left[D_B\bar{T}_y\bar{C}_y + \frac{D_T}{\bar{T}_\infty}\left(\bar{T}_y\right)^2\right] \tag{8}$$

Consider the following similarity transformation [40]

$$\eta = \sqrt{\frac{y^2a_0e^{x/l}}{2\nu l}}, \bar{U} = a_0e^{x/l}f'(\eta),\ \bar{V} = -\sqrt{\frac{\nu a_0e^{x/l}}{2l}}\left[f(\eta) + \eta f'(\eta)\right] \tag{9}$$

$$\bar{T} = \bar{T}_\infty + \bar{T}_0e^{x/2l}\theta(\eta),\ \bar{C} = \bar{C}_\infty + \bar{C}_0e^{x/2l}\phi(\eta),\ \bar{N} = \bar{N}_\infty + \bar{N}_0e^{x/2l}\chi(\eta)$$

The similarity transformation has been applied in equations (1) to (5):

The same solution is found for Equation (1); the reduced ODE equations for equations (2) to (5) are given below in Equations (10) to (13)

Dimensionless momentum equation:

$$f''' - Mf' - 2f'^2 + ff'' + \lambda(\theta - Nr\phi - Rb\chi) = 0 \quad (10)$$

Dimensionless energy equation:

$$\left(1+\frac{4}{3}K\right)\theta'' + \Pr(f\theta' - \theta f') + \theta'(Nb\phi' + Nt\,\theta') = 0 \quad (11)$$

Dimensionless concentration equation:

$$\phi'' + \left[f\phi' - Cr\phi - \phi f' - \sigma_m\phi(1+\delta\theta)^n e^{\frac{-E}{1+\delta\theta}}\right]Sc + \frac{Nt}{Nb}\theta'' = 0 \quad (12)$$

Dimensionless bioconvection equation:

$$\chi''(\eta) + Lb\Pr f(\eta)\chi'(\eta) - LbPrf'(\eta)\chi(\eta) - Pe\left[\sigma_1\phi''(\eta) + \chi(\eta)\phi''(\eta) + \chi'(\eta)\varphi'(\eta)\right] = 0 \quad (13)$$

The associated boundary conditions become into

$$f'(0) = 1,\ f(0) = -s,\ \phi(0) = 1,\ \theta(0) = 1,\ \chi(0) = 1,\ at\ \eta = 0, \quad (14)$$

$$f'(\infty) \to 0,\ f''(\infty) \to 0,\ \phi(\infty) \to 0,\ \theta(\infty) \to 0,\ \chi(\infty) \to 0\ as\ \eta \to \infty$$

Along stretching surface, the shear stress τ_w, the thermal flux q_w, the mass flux q_m and the motile microorganisms flux q_n are as follows:

$$\tau_w = \mu\left[\bar{U}_y + \frac{\xi}{\sqrt{2}}\left(\bar{U}_y\right)^2\right]_{y=0},\ q_w = -\left[R + \frac{4\sigma^*\bar{T}_\infty^{\,3}}{k^*}\left(\frac{\partial\bar{T}}{\partial y}\right)\right]_{y=0}, \quad (15)$$

$$q_m = -D_B\left(\frac{\partial\bar{C}}{\partial y}\right)_{y=0},\ q_n = -D_N\left(\frac{\partial\bar{N}}{\partial y}\right)_{y=0}$$

The expression for C_{f_x}, Nu_x, Sh_x and Nn_x are as follows

$$C_{f_x} = \frac{\tau_w}{\rho\bar{U}_w^{\,2}},\ Nu_x = \frac{xq_w}{k\left(\bar{T}_w - \bar{T}_\infty\right)},\ Sh_x = \frac{xq_m}{D_B\left(\bar{C}_w - \bar{C}_\infty\right)} \text{ and } Nn_x = \frac{xq_n}{D_N\left(\bar{N}_w - \bar{N}_\infty\right)} \quad (16)$$

The non-dimensional form of C_{f_x}, Nu_x, Sh_x and Nn_x are as follows

$$C_{f_x} = \frac{1}{\sqrt{Re}_x}\left[f''(0) + \frac{\lambda}{2}\left(f''(0)\right)^2\right],\quad Nu_x = -\sqrt{Re_x}\left[1+\frac{4}{3}R\right]\theta'(0) \quad (17)$$

$$Sh_x = -\sqrt{Re_x}\ \phi'(0),\ \ Nn_x = -\sqrt{Re_x}\ \chi'(0)$$

Here, $Re_x = \frac{x\bar{U}_w}{\nu}$

3. Numerical Solution Approach Methods

The FDM, FVM, and FEM are the fundamental discretization techniques. However, during calculation, these methods required much more for the finding of the unknowns, but the R-K method with shooting techniques is a suitable method to solve flow problems related to ODEs. To put it briefly, boundary value issues are adequately, quickly, and exactly solved using the R-K technique. Because of its relative simplicity this numerical approach is therefore frequently used in applied science's nonlinear analysis.

4. Results and Discussions

Numerical solutions are found for the physical interpretations of the non-dimensional formulation of steady nanofluid MHD flow caused by the exponential stretched sheet in the presence of a bioconvection equation and chemical reaction with the related boundary conditions.

Figure 1 demonstrates the velocity distribution for many values of the magnetic field parameter M. It is noticed that when M increases, the velocity decreases. This indicates that high resistance to fluid motion and a high viscosity are produced by Lorentz's force, which results in a drop in velocity.

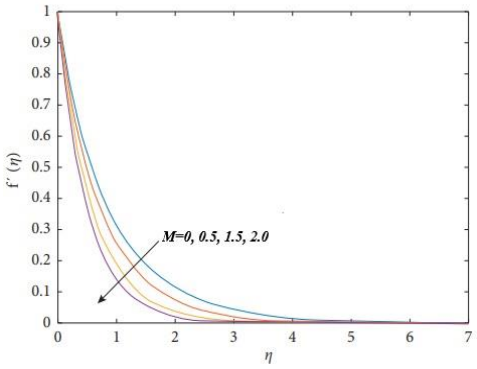

Figure 1: Repercussions of *M* values on $f'(\eta)$

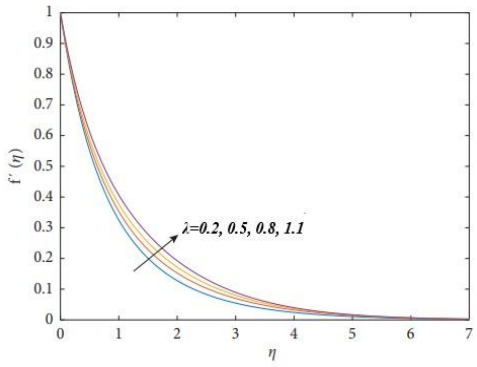

Figure 2: Repercussions of λ values on $f'(\eta)$

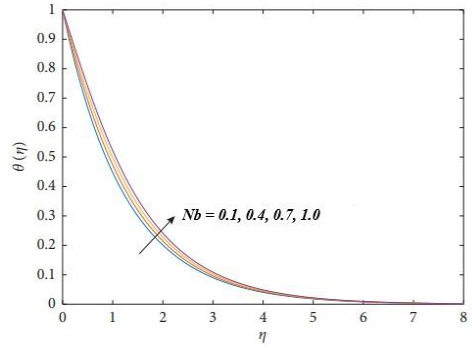

Figure 3: Repercussions of *Nb* values on $\theta(\eta)$

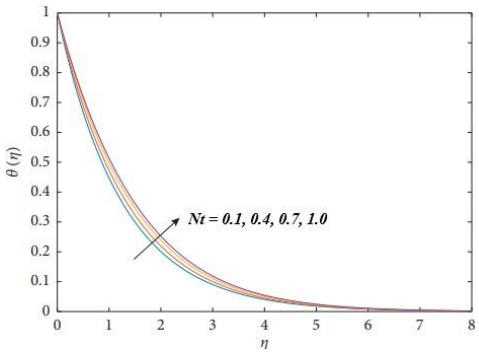

Figure 4: Repercussions of *Nt* values on $\theta(\eta)$

As seen in **Figure 2**, a rise in the mixed convection parameter λ results in an augmented in flow velocity $f'(\eta)$. With respect to the density variation and temp. gradient, the flow has a stronger buoyancy effect by the mixed convection. The fluid flow was improved by this phenomenon.

With increased values of the thermophoresis parameter *Nt* and the Brownian motion parameter *Nb*, **Figures 3 and 4** show a notable increasing behaviour of $\theta(\eta)$. The increased heat transfer to rise $\theta(\eta)$ is resulting from the quick, arbitrary movement of nanoparticles, that are identified by higher *Nb*. Comparably, an increase in *Nt* indicates a stronger thermophoretic impact, which shifts the hotter regime of the nanoparticles to the colder one and widens the thermal distribution.

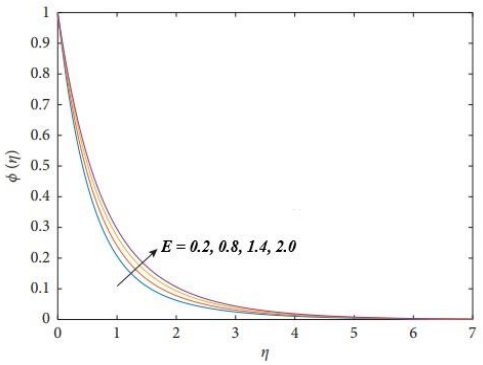

Figure 5: Repercussions of *E* values on ϕ

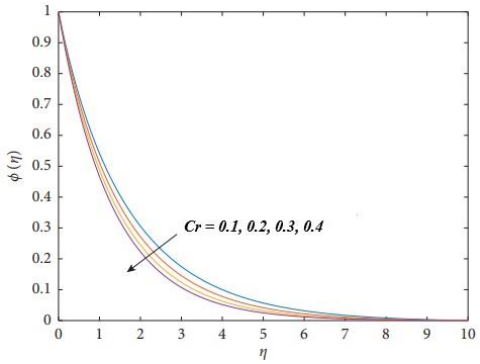

Figure 6: Repercussions of *Cr* values on ϕ

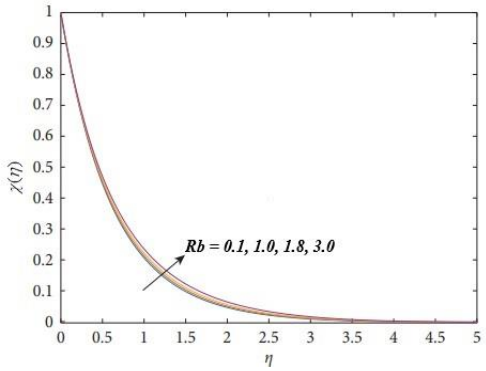

Figure 7: Repercussions of *Rb* values on $\chi(\eta)$

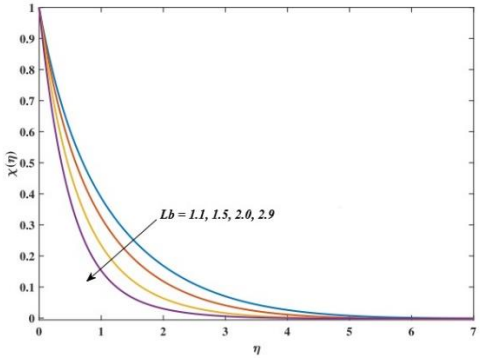

Figure 8: Repercussions of *Lb* values on $\chi(\eta)$

The concentration profile is influenced by A.E., as seen in **Figure 5**. There is an increase in *E*. In the end, the circumstances favor fluid substances that produce higher concentrations. Therefore, as the A.E. is increased, the density gradient rises.

The decrease in $\phi(\eta)$ that results from an increased value of the *Cr* is seen in **Figure 6**, where the chemical reaction speeds up to reduce the nanoparticles' concentration.

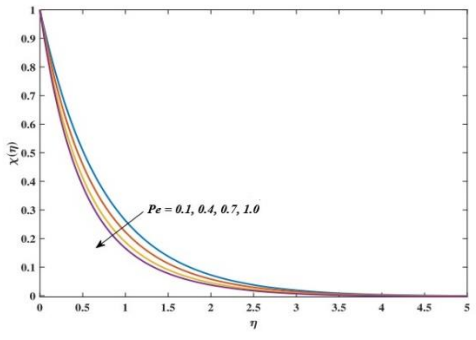

Figure 9: Repercussions of *Pe* values on $\chi(\eta)$

Figure 7 illustrates how the bioconvection Rayleigh number *Rb* is directly responsible for providing an increment of $\chi(\eta)$. As *Rb* rises, so does the density of the motile microbes.

The Bio. LN (*Lb*) of mobile bacteria is the product of their mass diffusivity with heat diffusivity. In biology or medicine, this gauge characterizes the heat transfer brought on by microorganisms. This feature is reversed near a free stream, where the motile microbe density decreases and the *Lb* value rises shown in **Figure 8**. Due to their ability to move independently, microorganisms induce a change in profile by reducing the amount of surface bioconvection.

Figure 9 illustrates how the dimensionless density of microorganisms decreases as the Peclet number (*Pe*) grows. A higher *Pe* value indicates a stronger pattern of microbial movement, which decreases the microorganism profile. This number quantifies the intensity of directed and random swimming in motile microorganisms.

Table 1 shows how several factors, including the Williamson fluid parameter *We*, magnetic field parameter *M*, suction/injection parameter *s*, and affect the skin friction coefficient. It is demonstrated that the $\sqrt{Re_x}C_{f_x}$ is decreased of the variations in the *We*. More fluid motion resistance can be produced by longer relaxation times when the Williamson fluid value is higher. Consequently, the coefficient of skin friction decreases.

Table 1: Impact of $\sqrt{Re_x}C_{f_x}$

We	***s***	***M***	$\sqrt{Re_x}C_{f_x}$ P. Priyadharshini et al [39]	**Present calculations**
0.1	0.2	2.0	1.7543	1.7537
0.2			1.6830	1.6765
0.3			1.6200	1.6198
	0.1		1.7976	1.7989
	0.2		1.7543	1.7537
	0.3		1.7123	1.7118
		0.1	1.2035	1.2018
		0.2	1.2383	1.2342
		0.3	1.2722	1.1699

It has been shown that a lower $\sqrt{Re_x}C_{f_x}$ is obtained with increased suction/injection parameter *s*. This suggests that higher fluid flow resistance is caused by an increase in the porosity of the stretched sheet. According to our study, $\sqrt{Re_x}C_{f_x}$ increases with rising the values of *M*. The speed at which fluid particles tend to flow is determined by the Lorentz force. At the surface level, there is an increase in $\sqrt{Re_x}C_{f_x}$.

Table 2: Impact of Nu_x

Pr	***K***	***Nt***	***Nb***	$Nu_x = -\theta'(0)$ P. Priyadharshini et al 391**]**	**Present calculations**
1.3	0.2	0.1	0.1	0.9475	0.9468
1.4				0.9881	0.9672
1.5				1.0271	0.9998
	0.2			0.9475	0.9468
	0.6			0.7731	0.7939
	1			0.6631	0.6781
		0.1		0.9475	0.9468
		0.4		0.8551	0.8677
		0.7		0.7617	0.7761
			0.1	0.9475	0.9468
			0.4	0.8435	0.8528
			0.7	0.7466	0.753

Table 2 illustrates how the radiation parameter *R* affects fluid temperature. The thermal boundary layer's width as well as the dispersion of rise as the values of the *R* do. The Rosseland radiative absorption is decreasing, which causes the radiative heat change to diverge more. As a consequence, the increase in the radiative heat transmission rate causes the fluid's temperature to rise. As an outcome, the Nu_x falls. Diffusion thermophoresis factor causes Nu_x to decrease. The hot zone's high energy levels and fluid molecular movement, which force the nanoparticles out of the area, are responsible for this phenomena. Heat transfer occurs more quickly when heated particles pass from the region of high temperature to the cold zone.

The fluid's energy increases as the Brownian motion factor *Nb* grows. This process illustrates the Brownian motion *Nb* increase, which describes the zigzag movement fluid particles. When there is a boost in Brownian motion, the value of Nu_x decreases substantially because there are more fluid particle collisions.

Table 3: Impact of Sh_x

σ_m	***E***	***Nt***	***Nb***	$Sh_x = -\phi'(0)$ P. Priyadharshini et al [39**]**	**Present calculations**
0.3	0.2	0.1	0.1	0.7528	0.7532
0.5				0.8807	0.8821
0.7				0.9923	0.9967
	0.2			0.7528	0.7532
	0.7			0.7338	0.7299
	1.3			0.7127	0.710
		0.1		0.7528	0.7532
		0.4		1.0846	1.0989
		0.7		1.1316	1.1441
			0.1	0.7528	0.7532
			0.2	0.3566	0.3788
			0.3	−0.0182	0.0005

Table 3 indicates that the Sh_x (Sherwood number) is a numerical depiction using several parameters, including σ_m, *E*, *Nt* and *Nb*.

The is evident the value of Sh_x increased when σ_m rises. Actually, the rate of reaction approaches the Burke-Schumann limit. The Sherwood number increases due to the lower species' diffusion coefficient.

It is seen that the value of Sh_x down when the dimensionless A.E. values are raises. This suggests that the rate of diffusion surpasses the rate of mass transfer as the Reynolds number increases. There is higher A.E. as the the lower Sh_x. A higher A.E. indicates that a more successful collision between the particles will need more energy.

An increase in the *Nb* results in an enhancement of values of Sh_x. Higher values of *Nb* are seen when the surface roughens due to an enhance in the mobile microorganisms' density and the Sh_x.

The value of Sh_x falls down as the values of the *Nt* increased. This is proven by the fact that, as the fractional derivative parameter increases, the temperature rises because the thermal resistance decreases. In terms of mechanics, the heat flux vector's phase lag and temperature gradients exhibit opposing trends.

Table 4: Impact of Nn_x

Pe	***Lb***	σ_1	$Nn_x = -\chi'(0)$ P. Priyadharshini et al [39]	**Present calculations**
0.1	1.1	0.1	1.1183	1.1187
0.4			1.2968	1.2979
0.7			1.4806	1.4837
	1.1		1.1183	1.1187
	1.4		1.2857	1.2875
	2.0		1.5740	1.5781
		0.1	1.1183	1.1187
		0.3	1.1270	1.1265
		0.5	1.1357	1.1342

The effects of Nn_x (mobile microorganisms) under various parameters, *Pe*, *Lb* and σ_1, are shown in Table 4.

We may investigate if a larger concentration of motile microorganisms with a higher Peclet Number (*Pe*) could be advantageous. It is obvious that the interaction of rotational and magnetic fields significantly increases microbial movement. This increase in velocity and concentration fields can be seen as a stretching influence that forms on the flow of plasma nanofluid containing bacteria.

The motile microbes improved as the Bio. LNo. values (*Lb*) enhanced. These results show that as the *Lb* rises, so does the motile bacterial density and that associated stress lowers as microorganisms move from the sheet over the boundary layer.

The quantity of motile microbes rises as the σ_1 (bio-convection difference parameter) varies more quickly. It is discovered that the motile bacteria's density minimizes as the *Pe* rises. Temperature and concentration are known to be primarily transmitted by changes in mass and heat, respectively

5. Conclusion

In the current study, MHD Williamson fluid flow has been analysed for an exponential stretching sheet by employing numerical approaches. The physical fields of temperature, velocity, and microbe distribution are the ones on which the results of the parameters are listed. The following significant results are summarized:

- The velocity of fluid gets enhanced with the mixed convection parameter (λ) and decreases with the magnetic parameter (*M*). This happens because Lorentz's force causes a high viscosity, which raises the Williamson fluid parameter and rises the resistance to fluid motion and the velocity profile.
- The Brownian motion (*Nb*), and the thermophoresis diffusion (*Nt*) resulted in a larger temperature distribution due to the rapid and random motion of the nanoparticles.
- With chemical reaction parameter (*Cr*), concentration recurs, and with A.E. parameter (*E*), it is enhanced.
- An increased Bio. LNo. and Peclet number resulted in a reduction in the microorganism profile. These indicates physical measurement of the relative strength and random motion in motile bacteria. Raising the Rayleigh number (bioconvection) *Rb* results in an enhanced motile microbe profile.

Nomenclature

Magnetic field parameter: $M = \dfrac{2\sigma {M_0}^2 l}{\rho \bar{U}_w}$

non-dimensional Williamson fluid parameter: $We = \xi \sqrt{\dfrac{\bar{U}_w^{\,3}}{l\nu}}$

suction/injection (s > 0/ s < 0) parameter: $s = \sqrt{\dfrac{2{V_0}^2 l}{a_0 \nu}}$

Mixed convection: $\lambda = \dfrac{2\beta\xi l(1-\bar{C}_\infty)(\bar{T}_w - \bar{T}_\infty)}{\bar{U}_w^{\,2}}$

Brownian motion factor: $Nb = \dfrac{\tau D_B \left(\bar{C}_w - \bar{C}_\infty\right)}{\nu}$

Buoyancy ratio factor: $Nr = \dfrac{(\rho_p - \rho_f)\left(\bar{C}_w - \bar{C}_\infty\right)}{\beta\rho(1-\bar{C}_\infty)(\bar{T}_w - \bar{T}_\infty)}$

Rayleigh number of bio-convection: $Rb = \dfrac{\gamma(\rho_m - \rho_f)\left(\bar{C}_w - \bar{C}_\infty\right)}{\beta\rho(1-\bar{C}_\infty)(\bar{T}_w - \bar{T}_\infty)}$

Thermophoresis diffusion: $Nt = \frac{\tau D_T \left(\bar{T}_w - \bar{T}_\infty\right)}{\nu \bar{T}_\infty}$

Rate of the reaction (Dimensionless): $\sigma_m = \frac{2K_r{}^2 l}{\bar{U}_w}$

Non-dimensional activation energy(A.E.): $E = \frac{Ea}{k\bar{T}_\infty}$

Bio-convectional difference parameter: $\sigma_1 = \frac{\bar{N}_\infty}{\bar{N}_w - \bar{N}_\infty}$

Distinct parameter of temperature: $\delta = \frac{\bar{T}_w - \bar{T}_\infty}{\bar{T}_\infty}$

Schmidt number: $Sc = \frac{\nu}{D}$

Peclet number: $Pe = \frac{dWc}{D_n}$

Bioconvection Lewis Number (Bio. LNo.): $Lb = \frac{\alpha}{D_n}$

Prandtl number: $\Pr = \frac{\nu}{\alpha}$

Radiation Parameter: $R = \frac{4\sigma^* \bar{T}_\infty{}^3}{k * k_f}$

M_0	Magnetic field coefficient	ν	Kinematic viscosity
$\bar{C}$	Concentration	k	Conductivity of heat
$\bar{T}$	Temperature	D_T	Thermophoretic diffusion coefficient
$\bar{N}$	Concentration of microorganisms	Φ	Concentration (Dimensionless)
Re	Reynold's number	q_r	Radiative heat flux
$\bar{T}_w$	Wall temperature	ρ	Density
$\bar{T}_\infty$	Temperature far away from the plate	α	Thermal diffusivity
$\bar{U}, \bar{V}$	Velocity components along x and y -axes	C_{f_x}	Skin friction coefficient
μ	Dynamic viscosity	Nu_x	Nusselt Number

Sh_x	Sherwood number	σ^*	Stefan-Boltzmann constant
Nn_x	Motile density number	k_1	Coefficient of Mean absorption

Refrences

[1] S.U. Choi and J.A. Eastman (1995), Enhancing thermal conductivity of fluids with nanoparticles, Argonne National Lab., IL (United States), Tech. Rep.

[2] Shahid, A.K.; Yufeng, N.; Bagh, A. (2019) Multiple Slip Effects on Magnetohydrodynamic Axisymmetric Buoyant Nanofluid Flow above a Stretching Sheet with Radiation and Chemical Reaction. Symmetry, 11, 1171.

[3] S.K. Das, S.U. Choi, W. Yu, T. Pradeep (2007) Nanofluids: science and technology, John Wiley & Sons.

[4] Islam, S.; Ur Rasheed, H.; Nisar, K.S.; Alshehri, N.A.; Zakarya, M. (2021) Numerical Simulation of Heat Mass Transfer Effects on MHD Flow of Williamson Nanofluid by a Stretching Surface with Thermal Conductivity and Variable Thickness Coatings, 11, 684.

[5] Ahmed, K.; Khan, W.A.; Akbar, T.; Rasool, G.; Alharbi, S.O.; Khan, I. (2021) Numerical Investigation of Mixed Convective Williamson Fluid Flow Over an Exponentially Stretching Permeable Curved Surface. Fluids, 6, 260.

[6] M. Khan, M. Malik, T. Salahuddin, A. Hussian,(2018) Heat and mass transfer of williamson nanofluid flow yield by an inclined Lorentz force over a nonlinear stretching sheet, Results in physics 8, 862–868.

[7] Ullah, Z.; Bilal, M.; Sarris, I.E.; Hussanan, A. (2022) MHD and Thermal Slip Effects on Viscous Fluid over Symmetrically Vertical Heated Plate in Porous Medium: Keller Box Analysis. Symmetry, 14, 2421.

[8] Kuznetsov, A.V. (2010) The onset of nanofluid bioconvection in a suspension containing both nanoparticles and gyrotactic microorganisms. Int. Commun. Heat Mass, 37, 1421–1425.

[9] Kuznetsov, A.V. (2011) Nanofluid bioconvection in water-based suspensions containing nanoparticles and oxytactic microorganisms: Oscillatory instability. Nanoscale Res. Lett., 6, 100.

[10] Khan, W.; Makinde, O.; Khan, Z. (2014) MHD boundary layer flow of a nanofluid containing gyrotactic microorganisms past a vertical plate with Navier slip. Int. J. Heat Mass Transf., 74, 285–291.

[11] Makinde, O.; Animasaun, I. (2016) Bioconvection in mhd nanofluid flow with nonlinear thermal radiation and quartic autocatalysis chemical reaction past an upper surface of a paraboloid of revolution. Int. J. Therm. Sci., 109, 159–171.

[12] Lu, D.; Ramzan, M.; Ullah, N.; Chung, J.D.; Farooq, U. (2017) A numerical treatment of radiative nanofluid 3D flow containing gyrotactic microorganism with anisotropic slip, binary chemical reaction and activation energy. Sci. Rep., 7, 17008.

[13] O. D. Makinde, (2005) Free convection flow with thermal radiation and mass transfer past a moving vertical porous plate, International Communications in Heat and Mass Transfer, vol. 32, no. 10, pp. 1411–1419.

[14] M. Sajid and T. Hayat (2008) Influence of thermal radiation on the boundary layer flow due to an exponentially stretching sheet, International Communications in Heat and Mass Transfer, vol. 35, no. 3, pp. 347–356.
[15] M. Abd El-Aziz (2009) Viscous dissipation effect on mixed convection flow of a micropolar fluid over an exponentially stretching sheet, Canadian Journal of Physics, vol. 87, no. 4, pp. 359–368.
[16] A. Ishak (2011) MHD boundary layer flow due to an exponentially stretching sheet with radiation effect, Sains Malaysiana, vol. 40, no. 4, pp. 391–395.
[17] R. N. Jat and G. Chand (2013) MHD flow and heat transfer over an exponentially stretching sheet with viscous dissipation and radiation effects, Applied Mathematical Sciences, vol. 7, no. 4, pp. 167–180.
[18] B. Shankar Goud, P. Srilatha, P. Bindu, and Y. Hari Krishna (2020) Radiation effect on MHD boundary layer flow due to an exponentially stretching sheet, Advances in Mathematics: Scientific Journal, vol. 9, no. 12, pp. 10755–10761.
[19] G. R. Rajput, B. P. Jadhav, and S. N. Salunkhe (2020) Magnetohydrodynamics boundary layer flow and heat transfer in porous medium past an exponentially stretching sheet under the influence of radiation, Heat Transfer, vol. 49, no. 5, pp. 2906–2920.
[20] B. K. Swain, B. C. Parida, S. Kar, and N. Senapati, (2020) Viscous dissipation and joule heating effect on MHD flow and heat transfer past a stretching sheet embedded in a porous medium, Heliyon, vol. 6, no. 10, p. e05338.
[21] N. S. A. Ismail, A. S. Abd Aziz, M. R. Ilias, and S. K. Soid (2021) MHD boundary layer flow in double stratification medium, Journal of Physics: Conference Series IOP Publishing, vol. 1770, no. 1, p. 12045.
[22] N. N. Reddy, V. S. Rao, and B. R. Reddy (2021) Chemical reaction impact on MHD natural convection flow through porous medium past an exponentially stretching sheet in presence of heat source/sink and viscous dissipation, Case Studies in Dermal Engineering, vol. 25, p. 100879.
[23] Chu, Y.M.; Khan, M.I.; Khan, N.B.; Kadry, S.; Khan, S.U.; Tlili, I.; Nayak, M. (2020) Significance of activation energy, bio-convection and magnetohydrodynamic in flow of third grade-fluid (non-Newtonian) towards stretched surface: A Buongiorno model analysis. Int. Commun. Heat Mass Transf. , 118, 104893.
[24] Mlamuli, D.; Hiranmoy, M.; Sibanda Sandile, S.M.; Sachin, S. (2022) A mathematical model for bioconvection flow with activation energy for chemical reaction and microbial activity. Pramana, 96, 112.
[25] Kumar, N.N.; Sastry, D.R.V.S.R.K.; Shaw, S. (2022) Irreversibility analysis of an unsteady micropolar CNT-blood nanofluid flow through a squeezing channel with activation energy-Application in drug delivery. Comput. Methods Programs Biomed., 226, 107156.
[26] Zafar, S.S.; Ayman, A.; Zaib, A.; Ali, F.; Faizan, M.; Abed Ahmed, M.; Samia, E.; Ijaz Khan, M. (2023) Simulation of Prandtl nanofluid in the mixed convective flow of activation energy with gyrotactic microorganisms: Numerical outlook features of micro-machines. Micromachines, 14, 559.

[27] Shahid, A.; Huang, H.L.; Bhatti, M.M.; Marin, M. (2022) Numerical computation of magnetized bioconvection nanofluid flow with temperature-dependent viscosity and Arrhenius kinetic. Math. Comput. Simul., 200, 377–392.

[28] Shaw Samantaray, S.S.; Misra, A.; Nayak, M.K.; Makinde, O.D. (2022) Hydromagnetic flow and thermal interpretations of Cross hybrid nanofluid influenced by linear, nonlinear and quadratic thermal radiations for any Prandtl number. Int. Commun. Heat Mass Transf., 130, 105816.

[29] Satya, S.S.S.; Mahato, R.; Sachin, S.; Mrutyunjay, D. (2023) Simulation of entropy and heat and mass transfer in Water-EG based hybrid nanoliquid flow with MHD and nonlinear radiation. Int. J. Comput. Methodol, 1–15.

[30] Oyelakin, I.S.; Sithole Mthethwa, H.; Peri, K.; Shaw, K.S.; Sibanda, P. (2022) Entropy generation optimization for unsteady stagnation Casson nano fluid flow over a stretching sheet with binary chemical reaction and Arrhenius activation energy using the bivariate spectral quasi-linearisation method. Int. J. Ambient Energy, 43, 6489–6501.

[31] Nawaz, M.; Naz, R.; Awais, M. (2017) Magnetohydrodynamic axisymmetric flow of Casson fluid with variable thermal conductivity and free stream. Alex. Eng. J., 7, 2043–2050.

[32] Miroshnichenko, I.V.; Sheremet, M.A.; Pop, I.; Ishak, A. (2017) Convective heat transfer of micropolar fluid in a horizontal wavy channel under the local heating. Int. J. Mech. Sci., 128, 541–549.

[33] Ibrahim, S.M.; Kumar, P.V.; Lorenzini, G.; Lorenzini, E.; Mabood, F. (2017) Numerical study of the onset of a chemical reaction and heat source on dissipative MHD stagnation point flow of Casson nanofluid over a nonlinear stretching sheet with velocity slip and convective boundary conditions. J. Eng. Thermophys., 26, 256–271.

[34] Turkyilmazoglu, M. (2017) Mixed convection flow of magnetohydrodynamic micropolar fluid due to a porous heated/cooled deformable plate: Exact solutions. Int. J. Heat Mass Transf., 106, 127–134.

[35] Ibrahim, S.M.; Lorenzini, G.; Kumar, P.V.; Raju, C.S.K. (2017) Influence of chemical reaction and heat source on dissipative MHD mixed convection flow of a Casson nano fluid over a nonlinear permeable stretching sheet. Int. J. Heat Mass Transf., 111, 346–355.

[36] Muhammed, I.A.; Muhammed, Z.; Mustafa, I.; Dumitru, B.; Bandar, A. (2022) Impact of Activation Energy and MHD on Williamson Fluid Flow in the Presence of Bio-convection. Alex. Eng. J., 61, 8715–8727.

[37] Ahmed, K.; Akbar, T. (2021) Numerical investigation of magnetohydrodynamics Williamson nano fluid flow over an exponentially stretching surface. Adv. Mech. Eng., 13, 16878140211019875.

[38] Goud, B.S.; Srilatha, P.; Bindu, P.; Krishna, Y.H. (2020) Radiation effect on mhd boundary layer flow due to an exponentially stretching sheet. Adv. Math. Sci. J., 9, 10755–10761.

[39] P. Priyadharshini, V. Karpagam, Nehad Ali Shah, and Mansoor H. Alshehri (2023) Bio-Convection Effects of MHD Williamson Fluid Flow over a Symmetrically Stretching Sheet: Machine Learning. Symmetry, 15, 1684. https://doi.org/10.3390/sym15091684

[40] Muhammad Imran Asjad, Muhammad Zahid, Fahd Jarad, and Abdullah M. Alsharif, (2022) Bioconvection Flow of MHD Viscous Nanofluid in the Presence of Chemical Reaction and

Activation Energy, Mathematical Problems in Engineering, Article ID 1707894, https://doi.org/10.1155/2022/1707894

[41] Muhammad Imran Asjad, Muhammad Zahid, Bagh Ali, and Fahd Jarad (2022) Unsteady MHD Williamson Fluid Flow with the Effect of Bioconvection over Permeable Stretching Sheet, Mathematical Problems in Engineering, Article ID 7980267, https://doi.org/10.1155/2022/7980267

[42] S. Shateyi and H. Muzara (2020) On the numerical analysis of unsteady MHD boundary layer flow of Williamson fluid over a stretching sheet and heat and mass transfers, Computation, vol. 8, no. 2, p. 55.